Structural and optical properties of nebulizer spray coated Ga: ZnO nanocrystalline thin films

V.Kalaiselvi[a] , K.Dhanakodi[b], K.Shanmugasundaram[b] , P.Thirunavukkarasu[b], R.Mathammal[c].

a) Department of Physics, Navarasam Arts and Science for women, Erode, Tamilnadu, India.
b) Department of Electronics, Sri Ramakrishna Mission Vidyalaya College of Arts and Science, coimbatore-641 020, Tamilnadu, India.
c) Department of Physics, Sri Sarada College for women, Salem, Tamilnadu, India.
corresponding Author (V.Kalaiselvi)
E-mail: **nk.arthi.kalai@gmail.com**

Abstract

Transparent thin films of Ga-doped ZnO (GZO), with Ga dopant levels that varied from 0 to 5%, were deposited onto glass substrates by nebulizer spray technique. Sprayed film was temperature at 400 °C for 10 min with different Ga concentrations. The effects of Ga dopant concentrations on crystallinity levels, microstructures, and optical properties, of these ZnO thin films were systematically investigated. XRD results revealed that pure ZnO thin films exhibited a ideal orientation along the (002) plane and Ga doped ZnO thin films showed better crystallinity. HRSEM micrographs showed that all the films have two-form grains, vertically grown hexagonal and nanorods. Measurement and energy-dispersive X-ray spectroscopy (EDX) proved that the ZnO thin films on the GZO thin films deposited at higher substrate temperature had less defects and were closer to stoichiometric ZnO. The optical transmittance measurements show that all films are highly transparent in the visible wavelength region with an average transmittance of about ~72-82%. Photoluminescence spectra of GZO thin films were examined at room temperature.

Keywords: Thin films; Electron microscopy; X-ray diffraction; Optical properties;

1. Introduction

Transparent conducting oxide (TCO) ZnO thin films are emerging as the most attractive alternative to ITO and various other TCOs [1–4]. ZnO has traditional significant interest for its potential applications in gas sensors, UV light emitters, spin functional devices, transparent

electronics and surface acoustics wave devices. During synthesis of thin films, introducing impurities such as In, Al, Ga, N, P, As and F [5], within ZnO thin films is a common practice to enhance the optoelectronic properties. ZnO : Ga (GZO) thin films have been deposited by various techniques such as MBE(molecular beam Epitaxy) [6], Pulsed laser deposition [7], sintering [8], chemical spray pyrolysis [9, 10], RF magnetron sputtering [11], ion plating [12] and solid state reaction [13]. Photoluminescence (PL) and photocurrent measurements were carried out to study the emission and absorption properties of the Ga-doped ZnO film [6]. Both the spectra were constant with each other viewing a good reaction in the ultraviolet region and weak reaction in the green–yellow band. A structural and electrical property depends on the thickness of polycrystalline Ga-doped ZnO thin films prepared by reactive plasma deposition [7] were reported. The structural and electrical property of the GZO films was inducing changes when thickness was below 100 nm. Raman spectroscopy was used to study structural properties [12] of Ga-doped ZnO thin films synthesized at various oxygen partial pressures by the ion plating method. Raman spectra revealed the local vibrational modes associated with Gallium and Zinc, signifying that main defect species were Ga, Zn and VO in GZO films. The chemical spray pyrolysis technique is simple, low cost and can be used effectively for large area deposition and film properties can be tailored by controlling the spraying conditions.

In this paper, ZnO thin films doped with different elements have been prepared using nebulizer spray pyrolysis technique. The effects of different doping elements on the structural, morphological, and optical properties of ZnO films are studied and discussed.

2. Experimental Details

The undoped and Ga doped ZnO thin films were prepared by nebulizer spray pyrolysis technique. The chemicals used for the preparation were analytical reagent grade (99.5% purity procured from S.D fine chemicals, Mumbai) zinc chloride [$ZnCl_2$], Gallium III chloride ($GaCl_3$) and methanol. The undoped and Ga doped ZnO thin films deposited on glass substrates at 400 ^oC with different Ga concentrations through by nebulizer spray pyrolysis technique. The working solution of 0.1 M $ZnCl_2$ was obtained by dissolving 0.548 g of $ZnCl_2$ diluted in 25 ml of methanol and deionized water (3:1) and second working solution of 0.1 M $GaCl_3$ in 25 ml of deionized water. Gallium (III) chloride was added to starting solution as a dopant. The Ga dopant level was defined by the Ga/(Ga+Zn) ratio; it varied from 0 to 5%. The initial solution was

uniformly mixed and obtained final solution was sprayed. The distance between the nozzle and substrate was set to 5 cm. During the spraying process, the substrates were heated by electrically heating the iron plate. The flow of the solution was 0.5 ml/min and air used as a carrier gas. Iron Constant thermocouple was used to control the Substrate temperature. The obtained film was allowed to cool after deposition at room temperature.

3. Results and Discussion

3.1 Structural properties of Ga doped ZnO films

X-ray diffraction patterns of the Ga doped ZnO films deposited at a substrate temperature 400^{o}C with different Y doping concentrations (x) is displayed in Fig. 3.1. It is observed that the diffraction peaks at 2θ^{o}=31.7^{o}, 34.4^{o}, 36.2^{o}, 47.5^{o}, 56.6^{o}, 62.8^{o}, 67.9^{o}, 69.0^{o} and 72.5^{o} corresponding to (100), (002), (101), (102), (110), (103), (112), (201) and (004) planes. The comparison of observed X-ray diffraction patterns with the standard Joint Committee for Powder Diffraction Standards (JCPDS) data (89-7102) confirms that the films are having hexagonal crystal structure with highly preferential orientation along [002] direction. Other orientations correspond to [100] and [101] directions are present with low relative intensities as compared to that of [002] direction, which indicates the preferred growth direction along c-axis. However, Mahdhi et al., [13] and Ji-Hong Kim et al.,[14] have found [002] as a preferred orientation for their films of ZnO obtained by using spray pyrolysis technique. No diffraction peaks of other impurity phases are found in those films.

The peak shift for hexagonal (002) plane of Ga doped ZnO films at 400^{o}C with different yttrium doping concentrations (x) are shown in Fig.3.1. It can be seen that the peak position corresponding to the preferential orientation along (002) plane is shifted to lower scattering angle (2θ^{o}) side when yttrium is incorporated. The lattice constants ‘a’ and ‘c’ were calculated by using the following expression.

$$\frac{1}{d^2} = \frac{4}{3}\left[\frac{h^2 + hk + k^2}{a^2}\right] + \frac{l^2}{c^2} \qquad (1.1)$$

The values of lattice constants ‘a’ and ‘c’ of the films are listed in Table.3.1. It is observed that (Table.1) the lattice constants ‘a’ and ‘c’ values are in good agreement with the standard values taken from JCPDS data card (89-7102).

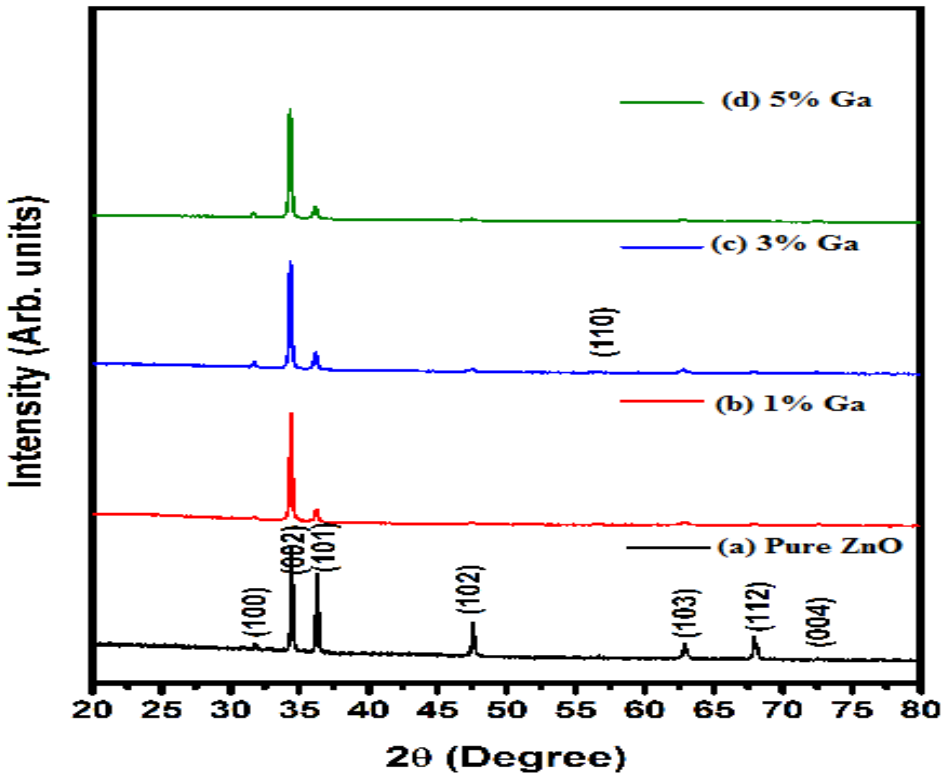

Fig.3.1 X-Ray diffraction patterns of Pure and Ga doped ZnO thin films

Besides, the lattice constants 'a' and 'c' values are found to be increased with yttrium doping concentration (x), which may be due to the higher ionic size of yttrium (r_{Gd}^{3+}= 0.09 nm) than that of zinc (r_{Zn}^{2+}=0.074 nm). The XRD was used to calculate the crystallite size (D) with the help of Scherrer's relation [15].

$$D = \frac{k\lambda}{\beta \cos\theta} \qquad (1.2)$$

Table.3.1 Calculated structural parameters of pure and Ga doped ZnO thin films

Nature of the films	2θ	d-spacing [Å]	FWHM [°2Th.]	(hkl) crystal System	Lattice constants		Scherrer	Dislocation Density, δ (10^{14}lin/m^2)	Micro Strain, ε (10^4 lin^{-2}m^{-4})
					(a x Å)	(c x Å)	Crystallite Size (nm)		
Pure	31.741	2.819	0.149	100	3.2497	5.2018	58	2.97	6.25
	34.36	2.609	0.168	002			57	3.74	7.00
	36.176	2.483	0.112	101			78	1.64	4.64
	47.471	1.913	0.091	102			100	1.00	3.63
	56.525	1.628	0.448	110			21	22.62	17.2
1%Ga	31.716	2.821	0.149	100	3.2499	5.2102	58	3.01	5.87
	34.364	2.607	0.114	002			76	1.72	4.10
	36.231	2.477	0.205	101			43	5.53	6.99
	47.495	1.912	0.319	102			28	12.4	8.08
	56.635	1.623	0.547	110			17	33.7	11.3
3%Ga	31.700	2.822	0.112	100	3.2540	5.2117	77	1.69	4.40
	34.332	2.612	0.112	002			77	1.67	4.05
	36.167	2.483	0.187	101			47	4.59	6.38
	47.532	2.912	0.224	102			40	6.13	5.68
	56.530	1.627	0.224	110			42	5.68	4.65
5%Ga	31.697	2.822	0.149	100	3.2543	5.2131	58	3.01	5.87
	34.319	2.612	0.112	002			77	1.67	4.05
	36.147	2.484	0.149	101			58	2.94	5.11
	47.404	1.917	0.261	102			35	8.34	6.64
	56.539	1.627	0.261	110			36	7.72	5.42

Where, k is the shape factor usually (k=0.94), λ is the X-ray wavelength and β is the full width in radian at half maximum of the peak and θ is the Bragg's angle of the X-ray diffraction peak. The values of crystallite size are listed in Table.1. The crystallite sizes of the all films are found to be in the range between 19 and 77 nm. The dislocation density and microstrain were calculated using equations (1.3) and (1.4) for the pure and Ga doped ZnO films [15].

$$\delta = \frac{1}{D^2} lines/m^2 \tag{1.3}$$

$$\varepsilon = \frac{\lambda}{D\sin\theta} - \frac{\beta}{\tan\theta} \tag{1.4}$$

The variation of dislocation density and microstrain with the different Y doping concentrations (x) are listed in Table.1. It observed that the dislocation density and micro strain for the (002) orientation plane decreases with the increase of Ga doping concentration from 0 to 5%, and the same may be due to the release of stress in the films. For 5% Ga doped film, the dislocation density and microstrain are found to be high. It has been concluded that the crystallinity of the films is higher for the lower values of dislocation density and microstrain.

3.2 Morphological analysis of Ga doped ZnO films

Typical high resolution scanning electron microscopy (HRSEM) images of the Ga doped ZnO thin films deposited at 400^{o}C with different Gallium doping concentrations (x) are shown in Fig. 3.2. No creaks are observed on large scan area of all films. As seen from the pictures, the grain size increases with gallium doping concentrations (x). The Figure 3.2a depicts thin films of undoped ZnO nanostructures consisting of uniform grains, tiny porous and vertically grown hexagonal shape crystal structure with an average thickness of 48 nm. For x=1% of Ga doping concentration of ZnO films seem to be covered by two-form grains, vertically grown hexagonal and nanorods with an average diameter ~38 nm is observed from Figure.3.2. When, gallium doping concentrations (x) increases from 3% to 5% (Figure.3.2), there are many hexagonal shaped particles which are irregular in size, very dense structured and well dispersed appear in the prepared films.

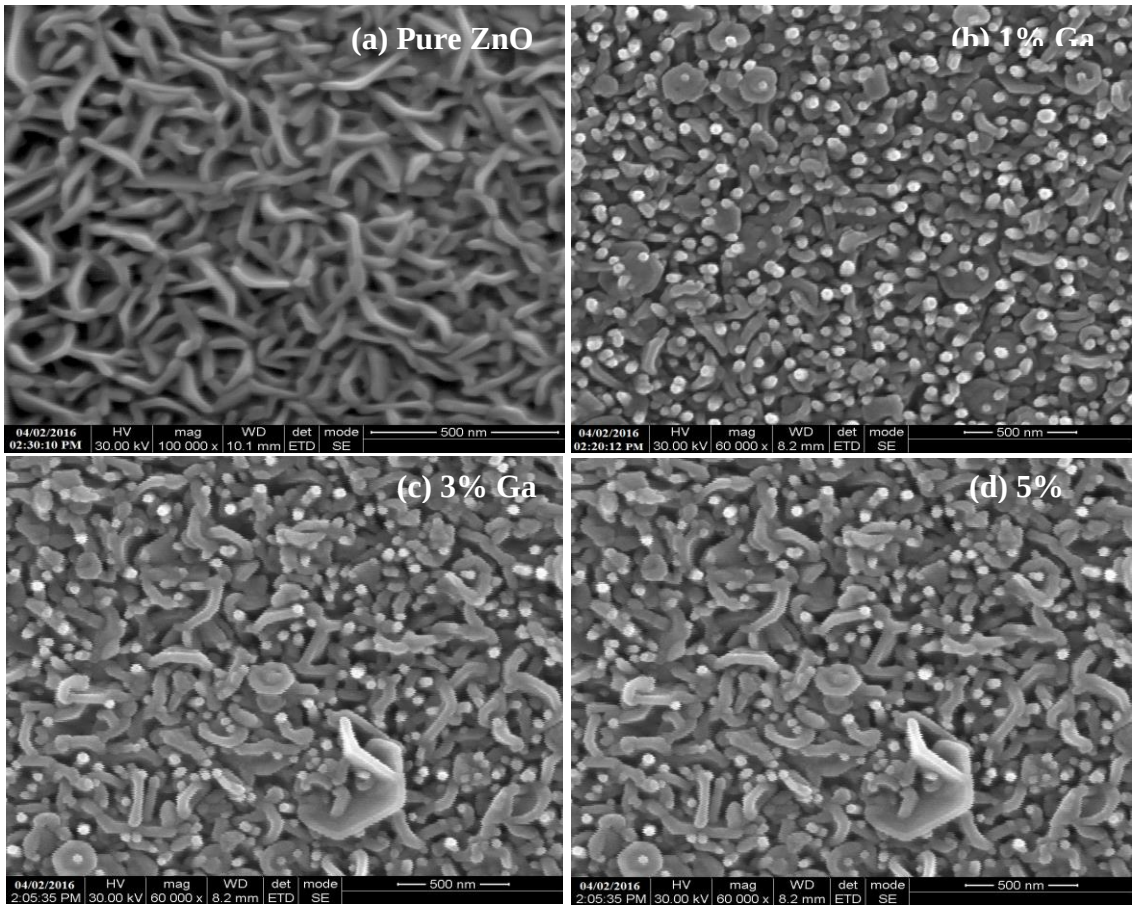

Fig.3.2 High resolution SEM images of Pure and Ga doped ZnO thin films

3.3 Elemental analysis of Ga doped ZnO films

The composition of films was confirmed by Energy dispersive X-ray spectroscopy. The EDAX spectra corresponding to qualitative and quantitative analysis of the Ga doped ZnO films deposited at 400^{o}C with different gallium doping concentrations (x) are shown in Fig.3.3. These spectra show the presence of expected elements Ga, Zn and O in the solid films. Other peaks reveal the existence of Ca and Si. These elements Si and Ca may probably be included from the glass which is used as substrate. It has seen from Fig.3.3 (insert Tables), increase in doping concentration leads to an increase in the atomic percentage of the dopant incorporated in the sample. It has been concluded that doping could be done very easily and effectively using spray pyrolysis technique.

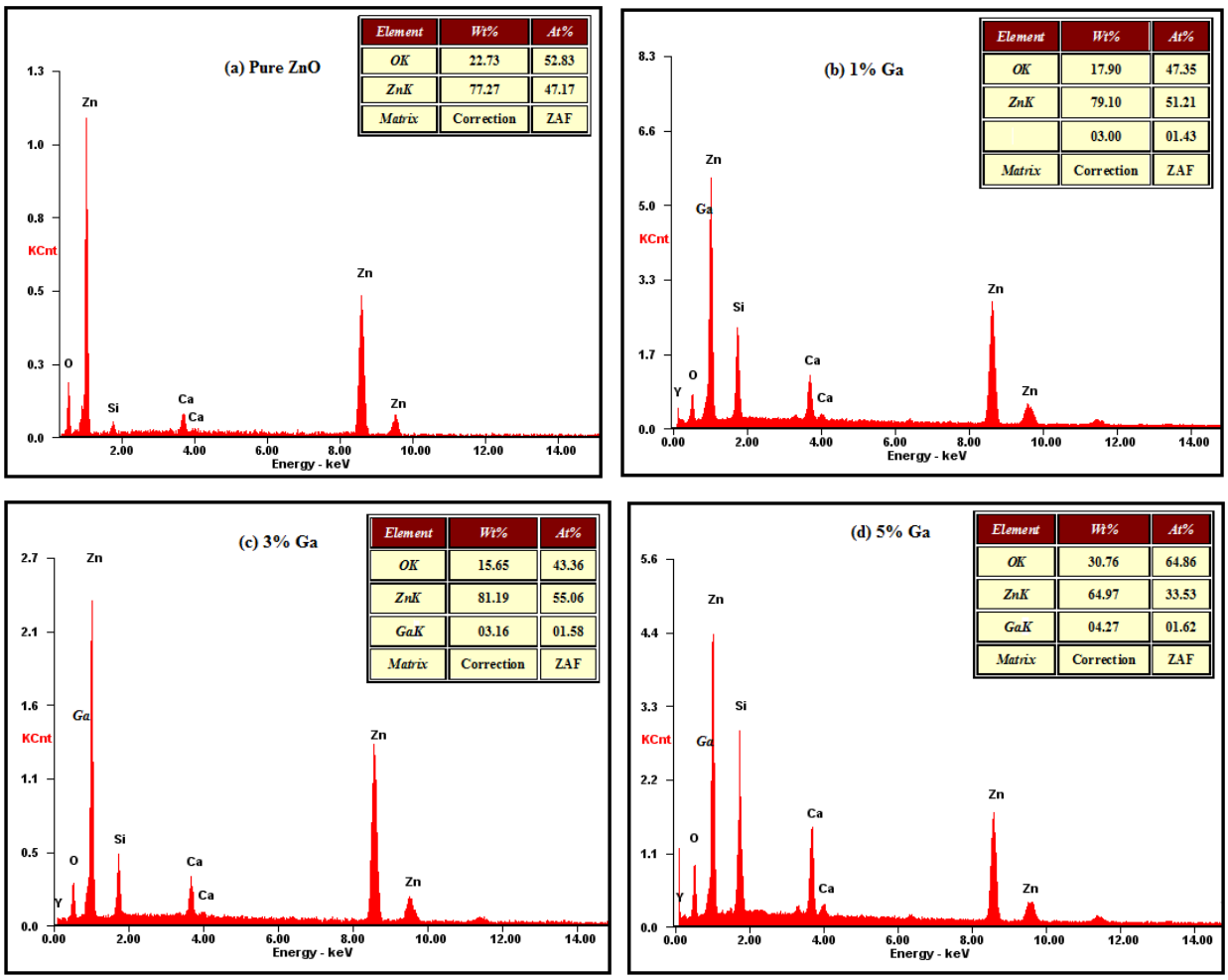

Fig. 3.3 EDAX spectra of Pure and Ga doped ZnO thin films

3.4 Optical properties of Ga doped ZnO films

The optical transmission in the UV-Vis-NIR region of pure and Ga doped ZnO films prepared at different gallium doping concentrations (x) with varied film thickness 350 nm, 330 nm, 318 nm and 310 nm through NSP technique is shown in Fig. 3.4. The transparency of the film decreases with the increase of the film thickness.

The films are highly transparent in the visible range with transmittance value changes from 72% to 82% and present a sharp ultra violet cut-off at ~390 nm. These results are in good agreement with values found for films with similar thickness. In this figure, edges shifted to shorter wavelengths (blue shifted) when Ga was incorporated into the ZnO films; these blue shifts may have been caused by doping induced film degradation [16]. It is observed that the

absorption edge shows a blue shift with yttrium doping concentration. The absorption coefficient 'α' was calculated from transmittance spectra using Beer-Lambert law [17];

$$\alpha = \frac{2.303x \log(1/T)}{t} \qquad 1.5$$

where, t is the film thickness, Since the Ga doped ZnO films fall in the family of direct transition semiconductors, λ is related to the optical energy gap by;

$$(\alpha h\nu)^2 = A(h\nu - Eg) \qquad 1.6$$

where, A is a constant, Eg is determined by extrapolating the straight line portion (αhν)=0, and hν is the photon energy, respectively. Fig.3.5 shows the Tauc's plot of $(\alpha h\nu)^2$ versus hν for Ga doped ZnO thin films. It is seen that the plot is linear over a wide range of photon energies indicates a direct band to band transition. The optical band gap (Eg) values increased from 3.04 to 3.19 eV as the Ga dopant values increased from 0 to 5% Ga. The band gap widening with dopant concentration is due to degraded crystallinity and reduced grain size [18-19].

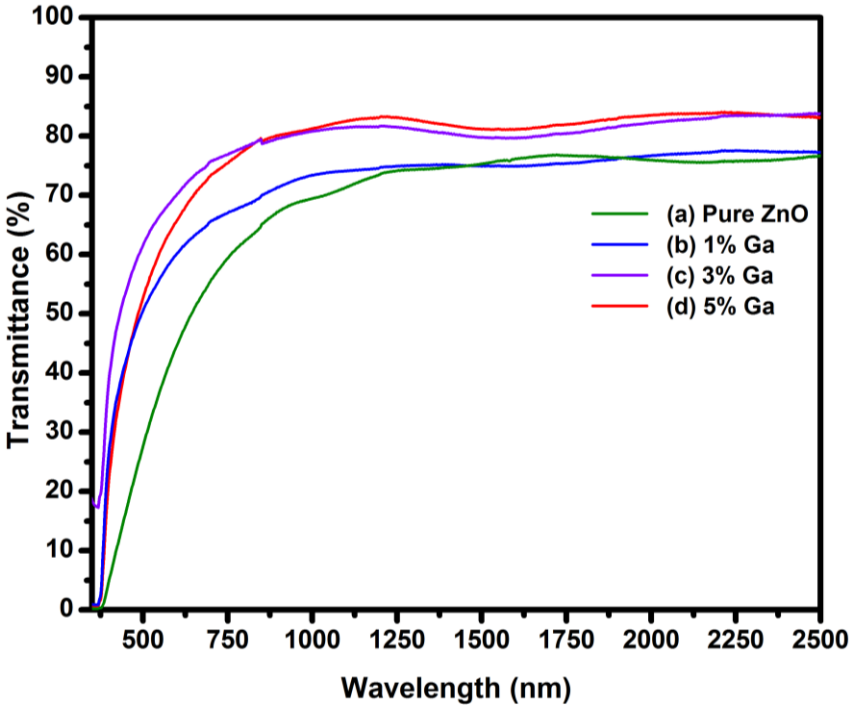

Fig.3.4 Transmittance spectra of Pure and Ga doped ZnO thin films

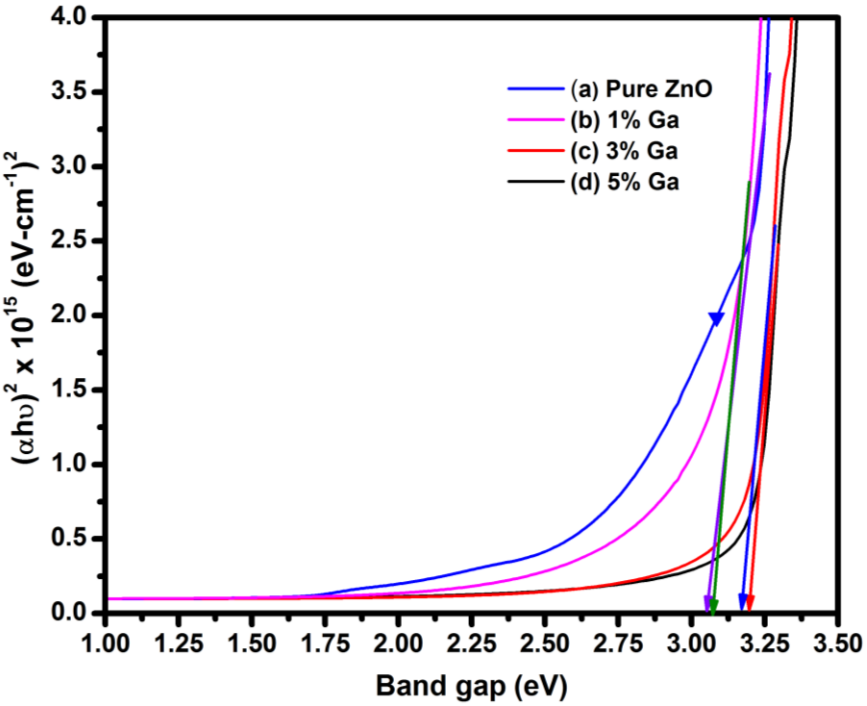

Fig. 3.5 $(\alpha h\upsilon)^2$ vs $(h\upsilon)$ plots for Pure and Ga doped ZnO thin films

3.5 Photoluminescence analysis of Ga doped ZnO films

Fig. 3.6 shows the room temperature photoluminescence spectra of pure and Ga doped ZnO thin films with different gallium doping concentrations (x).

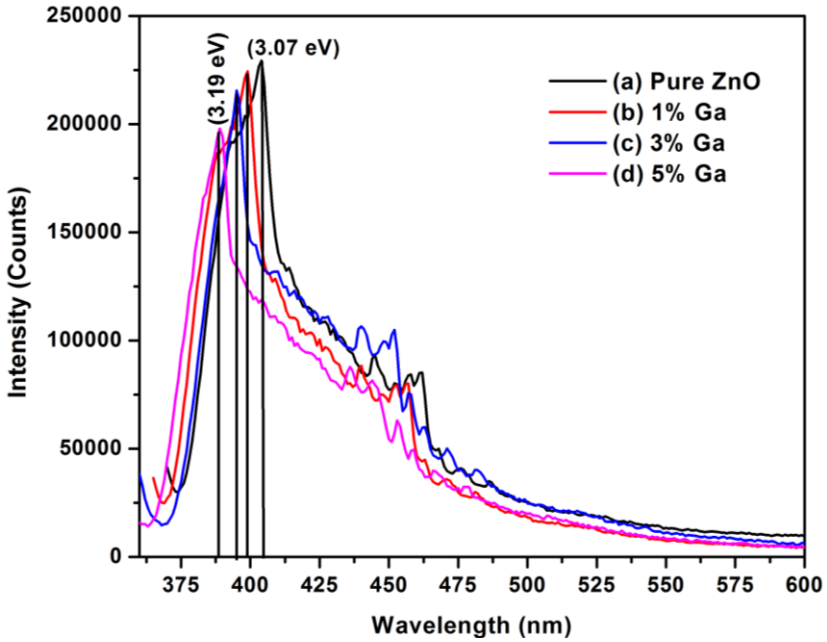

Fig.3.6 Room temperature PL spectra of Ga doped ZnO thin films

Each of PL spectra showed a broad double peak emission that combined a visible emission band and a weak ultraviolet emission band. The visible emission centers slightly shifted to shorter wavelengths as the Ga dopants increased from 0 to 5% Ga. The blue emissions might have been caused by intrinsic defects or dopant content. The emissions were preceded by electron transitions from Zn interstitial levels to the Zn vacancy levels [20].

4. Conclusion

The structural and optical properties of pure and Ga doped ZnO thin films deposited at a substrate temperature 400 ^{o}C with different gallium doping concentrations through the nebulizer spray pyrolysis technique were studied. The XRD spectra indicate that the Ga doped ZnO thin films are polycrystalline in structure with preferred orientation growth along (002) plane. The maximum crystallite size is found to be ~77 nm for the 5% Ga doped ZnO film. From the HR-SEM analysis of 1%Ga film, it is observed that the structure consists of nanorods with average diameter ~38 nm. The optical transmission of the Ga doped ZnO films is found to be increased with the increasing (x) values up to 5%Ga. The energy band gap varies from 3.04 to 3.19 eV as the doping concentration (x) changes from 0 to 7.5% and then increased for further changes.

.

References

[1] Dutta A and Basu S 1995 J. Mater. Sci.: Mater. Electron. 6 415–8

[2] Riad A S, Mahmoud S A and Ibrahim A A 2001 Physica B 296 319

[3] Tuzemen S, Gang Xiong, John Wilkinson, Brian Mischuck, Ucer K B and Williams R T 2001 Physica B 308 1197

[4] Zgur U, Alivov I Y, Liu C, Teke A, Reshchikov M A, Doan S, Avrutin V, Cho S-J and Morkoc¸ H 2005 J. Appl. Phys.98 041301

[5] Pearton S J, Norton D P, Ip K, Heo Y W and Steine T 2005 Prog. Mater. Sci. 50 293

[6] Mandalapu L J, Xiu F X, Yang Z and Liu J L, 2007 Solid State Electron. 51 1014–17

[7] Yamada T, Nebiki T, Kishimoto S, Makino H, Awai K, Narusawa T and Yamamoto T, 2007 Superlatt. Microstruct. 42 68–73.

[8] Ma Q B, Ye Z Z, He H P, Zhu L P, Wang J R and Zhao B H, 2007 Mater. Lett. 61 2460–3

[9] Kishimoto S, Hayashi K, Hamaguchi H, Makino H, Yamada T, Miyake A and Yamamoto T, 2007 Phys. Status Solidi b 244 1483–9

[10] Gomez H and Olvera M de la L, 2006 Mater. Sci. Eng. B 134 20–6

[11] Park S M, Ikegami T, Ebihara K and Shin P K, 2006 Appl. Surf. Sci. 253 1522–7

[12] Osada M, Sakemi T and Yamamoto T, 2006 Thin Solid Films 494 38–41

[13] H. Mahdhi, Z. Ben Ayadi, S. Alaya, J.L. Gauffier, and K. Djessas, Superlattics and Microstructures 72 (2014) 60-71.

[14] Ji-Hong Kim and In-Hyung Yer, Ceramics International 42 (2016) 3304-3308.

[15] R. Mariappan, V. Ponnuswamy, A. Chandra Bose, R. Suresh, and M. Ragavendar, Journal of Physics and Chemistry of Solids, 75 (2014) 1033-1040.

[16] J.H. Lee, K.H. Ko and B.O. Park, J. Cryst. Growth 247 (2003) 119.

[17] Jain, P. Sagar and R.M. Mehra, Solid State Electron. 50 (2006) 1420.

[18] R. Kaur, A.V. Singh, and R.M. Mehra, J. Non-Cryst. Solids 352 (2006) 2335.

[19] Bandyopadhyay, G.K. Paul, and S.K. Sen, Sol. Energy Mater. Sol. Cells 71 (2002) 103.

[20] X. Wei, B. Man, C. Xue, C. Chen and M. Liu, Jpn. J. Appl. Phys. 45 (2006) 8586.